100610 - 1002

DL/SRF/TM 10
(Instrumentation)

technical memorandum Daresbury Laboratory

DL/SRF/TM 10
(Instrumentation)

USE OF A DIAMOND CRYSTAL DETECTOR IN SYNCHROTRON RADIATION

by

J. H. POOLE
Daresbury Laboratory

MAY, 1977

Science Research Council

Daresbury Laboratory

Daresbury, Warrington WA4 4AD

1. INTRODUCTION

Diamonds have been used as radiation detectors for many years[1,2] but commercially produced detectors were not available until a few years ago. Most of the early work with diamonds was restricted to pulse detection with little use in the d.c. mode or as practical radiation monitors. The diamond crystal detector is a bulk conductivity device, that is, one in which the ionising radiation causes excitation of electrons to the normally unpopulated conduction band and the application of a polarising voltage allows collection of these electrons resulting in a current flow in an external circuit.

The work reported here was instigated because a device was required to scan the synchrotron radiation beam within the vacuum vessel of the NINA Synchrotron Radiation Facility (SRF). It was thought that a diamond would be a suitable detector and the purpose of the work was, therefore, to find the sensitivity and response of a diamond detector. With NINA operating at various energies the diamond was exposed to filtered synchrotron radiation. The amount of filtration was varied by using aluminium plates of various thicknesses to give a range of energy and intensity of the radiation striking the diamond.

The work established the working limits of the detector and gave an approximate value for the sensitivity. It was shown that the diamond is a suitable detector for the scanning device and subsequently such an instrument was designed.

2. EXPERIMENTAL DETAILS

The diamond was purchased from Electron Diamonds Ltd. of Hatton Garden, London. The detectors are manufactured in a variety of forms but

the one used in these experiments was encapsulated in epoxy resin and moulded onto the end of a miniature cable. The diamonds used are selected from normal gem stones on the basis of their electrical properties. Electrodes are attached to opposite faces of the diamond and a polarising voltage is applied across them.

The diamond used in this work had sides approximately 0.7 mm in length and was moulded within a cylinder of epoxy resin approximately 2.5 mm in diameter. Electrical connections to the diamond were via a miniature tri-axial cable, the connections being bias potential, signal collector and earthed screen. A negative polarising voltage was applied, the signal wire providing the current return via a pico-ammeter.

The diamond was exposed in the SRF on the x-ray table at the MRC window (fig. 1). The distance from the diamond to the tangent point in the synchrotron was 46.7 m and consequently the angle subtended by the diamond was very small ($\sim$ .015 mrad). The synchrotron light from the electron beam passed down the vacuum pipe into the SRF and out through a 0.4 mm thick beryllium window into the x-ray experimental area. The diamond was attached to a moveable collimator jaw so that it could be positioned vertically in the centre of the synchrotron radiation beam.

The bias supply and pico-ammeter were located as close to the diamond as possible, just outside the shield wall. This required a cable length of approximately 5 m from the instruments to the diamond. The fast rise time of the diamond ($\sim$ 10 ns) was degraded by this length of cable but since it was being used in the d.c. mode this was of no consequence.

The measurements were made during two 8 hour shifts separated by several weeks. Throughout both shifts absorber thicknesses and the beam current in NINA were varied (using the NINA control system to monitor the electron current). During the first shift the detector current was measured at various bias potentials for each absorber thickness. In the second shift all the measurements were made at one bias level. This second shift was to find any variation in sensitivity when the intensity was varied.

The aluminium absorbers were cut from foil and thin plate, enabling absorbers from 0.1 mm to 25 mm thick to be used. So that a wide range in absorber thickness could be covered conveniently, the increment of thickness was as close to the doubling thickness as possible. The absorbers were placed in the beam immediately in front of the diamond and secured for each measurement.

3. THEORY

The computation of the photon flux from NINA has been described in detail elsewhere[3,4,5] and this data was used as a starting point for the estimation of the flux falling on the diamond. The basic calculation of the power in the synchrotron radiation beam assumes that the beam acts as a point source. To estimate the practical situation the electron beam was assumed to have a Gaussian distribution with a vertical beam height of 1.5 mm (3 σ width).

This assumption about beam size is supported by measurements made on the synchrotron and by observation of the synchrotron radiation beam height. The observations, which have been made with radiation sensitive paper and by scanning with thin scintillators, indicate that the x-rays are confined to a region approximately 10 mm high at the beryllium window.

The mathematical description of the motion of electrons within the synchrotron is well known[6]. From the beam height at the tangent point it is possible to compute the angular deflection corresponding to an electron at any height. Since it was assumed that the beam had a Gaussian height distribution, the angular distribution within the beam is easily calculated. This information enables the effect of the finite beam height on the synchrotron radiation beam to be evaluated.

The absorption spectrum of aluminium is well known[7-10] and this was used to compute the intensity of the radiation passed by the filters. Thus:

$$p(\lambda,t) = P(\lambda) \cdot A(\lambda,t)$$

where p = power in the beam falling on the diamond

λ = wavelength

A = absorption factor

t = absorber thickness

P = incident beam power

This expression was integrated over wavelengths in the region of interest, for each of the absorber thicknesses, using a zero order trapezoidal integration. These results were compared with the observed detector currents for corresponding absorber thicknesses.

4. RESULTS

Figure 2 shows some typical bias curves obtained during the experiment. The curves indicate that the diamond exhibits saturation effects at the higher photon fluxes. The downward trend is probably the result of increased trapping of charge carriers within the crystal lattice, resulting in an electric field which opposes the polarising field, thus reducing collection efficiency. Since it was not possible to obtain more data in the time available no inference is drawn from the apparent variation in gradient of the curves. The large error bars are the result of uncertainties in reading meter scales in combination with beam current fluctuations.

Figure 3 shows the computed variation of the synchrotron radiation spectrum with absorber thickness. It can be seen that the principal effect of increasing the absorber thickness is to reduce the intensity of the radiation. To simplify the calculations it was assumed that the detector output current per unit power of radiation striking it was constant over this small wavelength range (0.15 to 1.5 Å).

The computed variation of the power falling on the diamond with absorber thickness is shown on fig. 4. Also plotted on fig. 4 are the normalised experimental data. The graph shows good agreement between the expected and observed detector currents indicating linearity in the detector response.

The computation of the absolute power falling on the diamond is subject to fairly large errors because of the uncertainty in some of the synchrotron parameters such as the beam size and position. The computation does indicate, however, that approximately 14000 erg s^{-1} per mA beam will fall on the sensitive area of the diamond detector when no absorber is present. This may be converted to a dose rate(11) and expressed in this way, the experiment indicates that a dose rate of 5.0×10^{8} rad hr^{-1} gave rise to a detector current of the order of 10^{-8} A with a 200 V bias.

5. CONCLUSIONS

The investigation showed that the diamond behaved in a linear fashion over a wide intensity range with biases between 100 V and 250 V. The sensitivity to soft x-rays (0.15 to 1.5 Å) was approximately 2×10^{-17} A per rad per hour with a 200 V bias.

It was shown that with high currents in NINA (> 14 mA) the diamond saturates when exposed to unfiltered radiation (this corresponds to a dose rate $\sim 10^{10}$ rad hr^{-1}). The inclusion of a thin filter (0.2 mm aluminium + 0.4 mm beryllium window) was sufficient to remove this effect. During the course of these and other experiments it is estimated that the diamond received a dose of the order of 10^{11} rad and was still functioning, with little deterioration in sensitivity. It is claimed by the manufacturers that the diamond detectors continue to function after receiving 10^{14} rad. It is likely that the slight deterioration in sensitivity observed in these experiments was due to radiation damage in the triaxial cable which was not made from radiation resistant materials. By using materials which are both radiation resistant and vacuum compatible, the diamond, with a suitable filter to prevent saturation, becomes well suited for use as a beam monitor within the vacuum system. The small physical size enables it to be used as a beam size and position indicator with good resolution and a synchrotron radiation beam scanning system utilising diamonds has been designed at Daresbury Laboratory.

The investigation has shown the diamond to be a useful diagnostic device in synchrotron radiation and because of their robustness, ease of use and low price it is likely that they will become increasingly important in this field.

REFERENCES

1. W. F. Cotty, Nature 177, (1956) 1075.
2. E. D. Wooldridge, A. J. Ahearn and J. A. Burton, Phys. Rev. 71, (1947) 913.
3. J. Schwinger, Phys. Rev. 75, (1949) 1912.
4. J. Poole, Daresbury Laboratory Internal Report, DL/SRF/TM1 (1975).
5. J. Poole, Daresbury Laboratory Internal Report, DL/SRF/TM6 (1976).
6. E. D. Courant and H. S. Snyder, Annals of Physics 3 (1958) p.1.
7. J. A. R. Samson, Techniques of vacuum ultraviolet spectroscopy, (New York: John Wiley, 1967).
8. D. J. Fabian, Soft x-ray band spectra, and the electronic structure of metals and materials, (London: Academic Press, 1968).
9. H. Enge, Introduction to Nuclear Physics, (Massachusetts, USA: Addison-Wesley, 1966) p.195.
10. R. C. Weast (Ed.), Handbook of Chemistry and Physics, 48th Edition (Cleveland, Ohio: Chemical Rubber Company, 1962) p.E-121.
11. U.S. Department of Health, Education and Welfare, Radiological Health Handbook, (Rockville, Maryland, 1970) p.132.

FIGURE CAPTIONS

1. Layout of the SRF.
2. Diamond detector current versus electron beam current for various bias levels.
3. Variation of the synchrotron radiation spectrum with absorber thickness. (a) 2.5 mm (b) 1.25 mm (c) 0.25 mm.
4. Computed variation of the power falling on the diamond with absorber thickness. Normalised experimental values ⧫

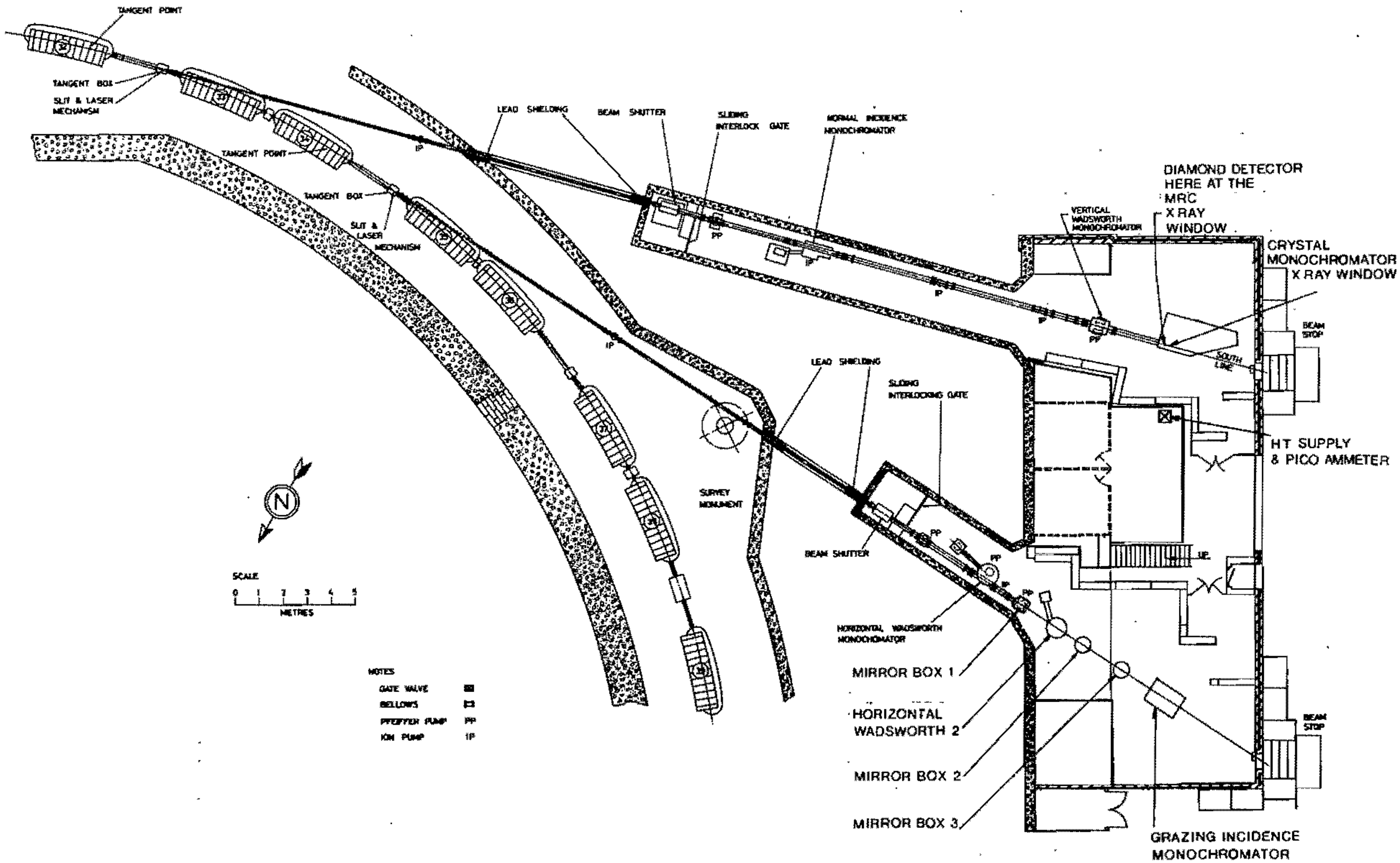
TANGENT POINT
TANGENT BOX
SLIT & LASER MECHANISM
TANGENT POINT
TANGENT BOX
SLIT & LASER MECHANISM
IP
LEAD SHIELDING
BEAM SHUTTER
SLIDING INTERLOCK GATE
NORMAL INCIDENCE MONOCHROMATOR
PP
IP
VERTICAL WADSWORTH MONOCHROMATOR
DIAMOND DETECTOR HERE AT THE MRC X RAY WINDOW
CRYSTAL MONOCHROMATOR X RAY WINDOW
BEAM STOP
SOUTH LINE
HT SUPPLY & PICO AMMETER
LEAD SHIELDING
SLIDING INTERLOCKING GATE
SURVEY MONUMENT
BEAM SHUTTER
PP
UP
HORIZONTAL WADSWORTH MONOCHROMATOR
MIRROR BOX 1
HORIZONTAL WADSWORTH 2
MIRROR BOX 2
MIRROR BOX 3
GRAZING INCIDENCE MONOCHROMATOR
BEAM STOP
SCALE
0 1 2 3 4 5
METRES
NOTES
GATE VALVE
BELLOWS
PFEIFFER PUMP PP
ION PUMP IP

Fig.1

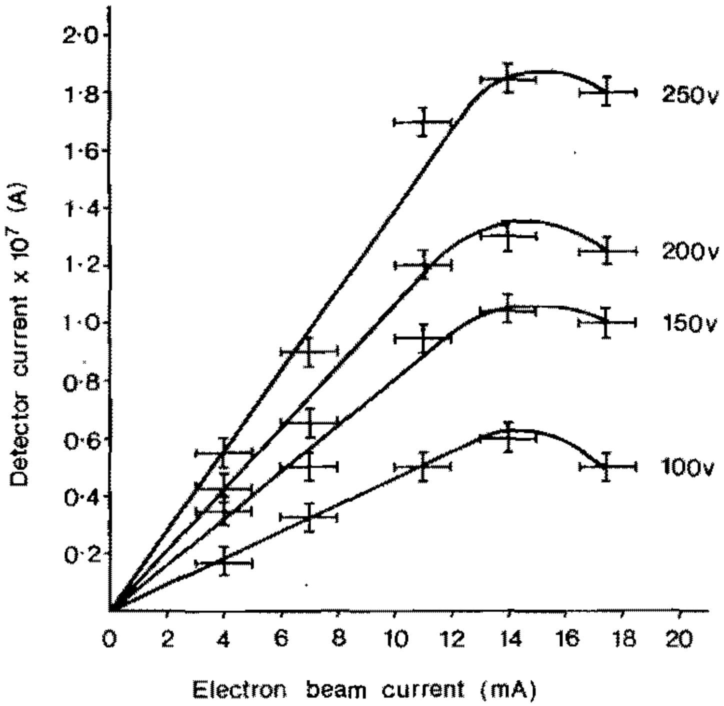
Detector current x 10^7 (A)
2·0
1·8
1·6
1·4
1·2
1·0
0·8
0·6
0·4
0·2
250v
200v
150v
100v
0 2 4 6 8 10 12 14 16 18 20
Electron beam current (mA)

Fig. 2

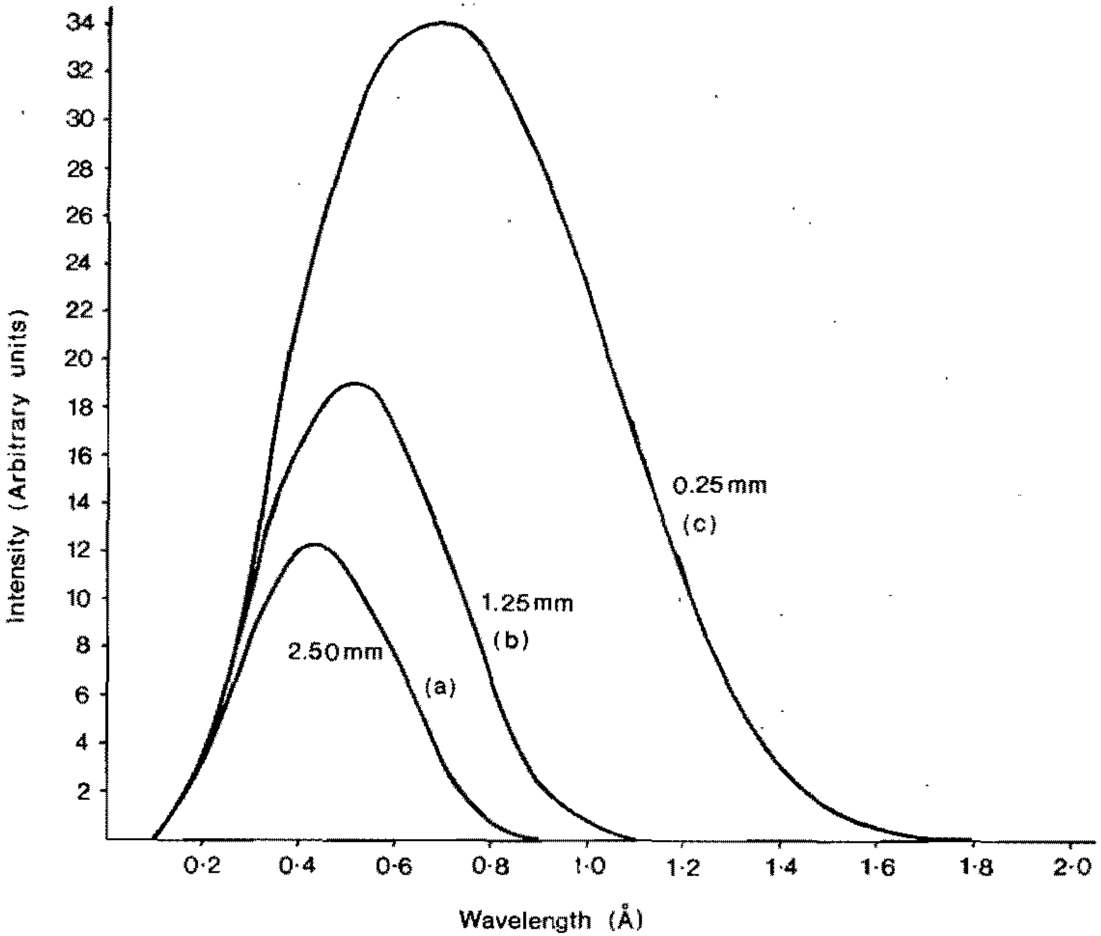
Intensity (Arbitrary units)
34 32 30 28 26 24 22 20 18 16 14 12 10 8 6 4 2
0.25mm
(c)
1.25mm
(b)
2.50mm
(a)
0·2 0·4 0·6 0·8 1·0 1·2 1·4 1·6 1·8 2·0
Wavelength (Å)

Fig. 3

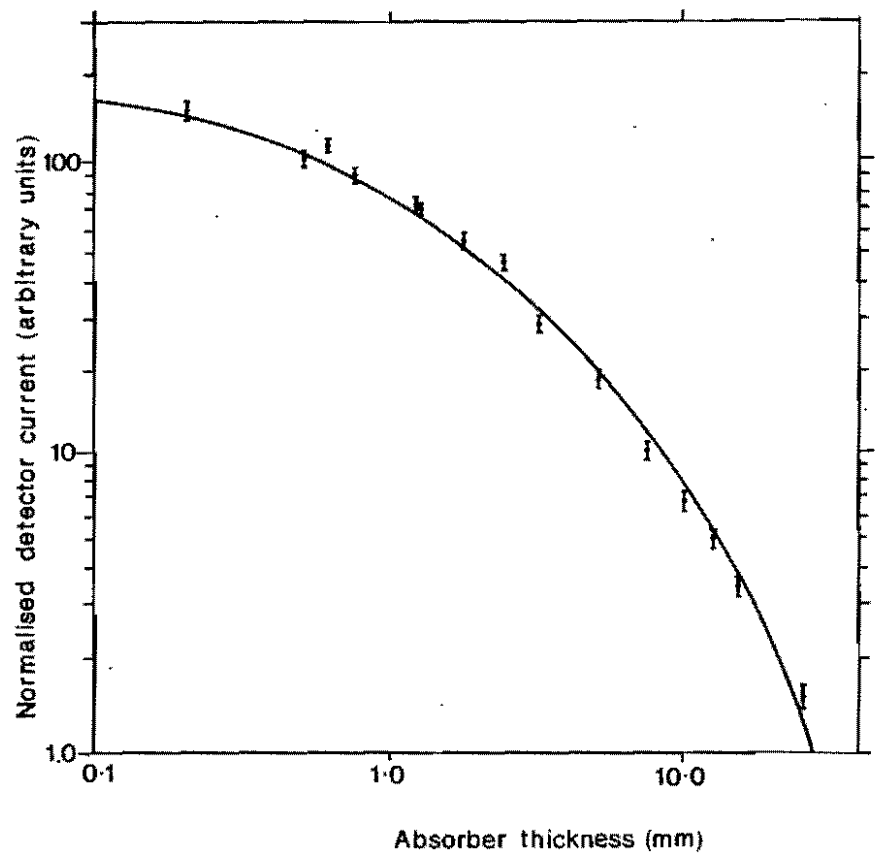
Normalised detector current (arbitrary units)
100
10
1.0
0·1
1·0
10·0
Absorber thickness (mm)

Fig. 4